Article

High-Yield, Environmentally-Friendly, and Sustainable Synthesis of Silver Nanowires Using Tannic Acid and Their Application in Conductive Ink Preparation: Economic Analysis and Rheological Investigation

Sina Kaabipour [1], Finley Neal [2], and Shohreh Hemmati [2,*]

[1] School of Chemical Engineering, Oklahoma State University, Stillwater, OK 74078, USA
[2] School of Mathematics and Natural Sciences, The University of Southern Mississippi, Hattiesburg, MS 39406, USA
* Correspondence: shohreh.hemmati@usm.edu
Received: 25 November 2024; Revised: 15 January 2025; Accepted: 11 February 2025; Published: 20 February 2025

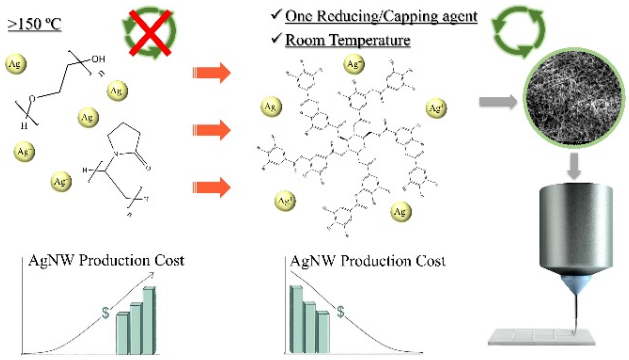

Abstract: Silver nanowires (AgNWs) have garnered significant attention during the past decade thanks to their applications in conductive inks used for electronic applications. The polyol process, widely used for AgNW synthesis, is known for its effectiveness in producing high aspect ratio and high yield nanowires. However, this process suffers from drawbacks such as high energy consumption and use of unsustainable reagents derived from non-renewable resources, which makes its large-scale utilization and economic feasibility challenging. In contrast, green synthesis methods offer potential solutions by employing environmentally friendly and cost-effective approaches. In this study, we offer a high-yield (90%) approach for the inexpensive, environmentally friendly, and sustainable synthesis of AgNWs, and show that the production cost per grams of AgNWs can be reduced by 31.72% compared to the polyol process. In addition, we investigate the rheological behavior of the synthesized AgNW-based conductive ink under screen printing and direct writing conditions using flow sweep, peak hold, and frequency sweep tests. The rheological behavior of the AgNW-based conductive ink provides valuable information regarding its use for various printing applications. The conductive ink demonstrated a shear-thinning thixotropic behavior for all silver nanostructure contents (2, 5, 10, and 20 wt.%), and all temperatures (25, 30, and 40 °C). It was observed that direct writing is better suited for printing inks with low colloidal content due to its lower shear rate, whereas screen printing is more effective for high-content, high-viscosity inks because it utilizes higher shear rates. The proposed cheaper and more sustainable method can serve as a promising alternative for industrial conductive ink manufacturing for printed electronic appliances such as printed circuit boards (PCBs) and flexible transparent conductive films (TCFs).

Keywords: silver nanowires; green chemistry; sustainability; rheology; conductive ink; screen printing; direct writing

1. Introduction

The development of metal-based colloidal conductive inks has gained significant attention for the manufacturing cost-effective, versatile, and flexible transparent conductive films (TCFs). These films have a wide range of applications, including wearable health-monitoring devices, supercapacitors, photodetectors, and solar cells, to name a few [1–4]. Indium tin oxide (ITO) is the most commonly used material for TCFs, due to its excellent optical transmittance (>90%) and its low sheet resistance (<10 Ω/square) [5]. However, its brittleness and energy-intensive manufacturing process limit its use in flexible electronics [5,6]. As an alternative, silver nanowire (AgNW)-based conductive inks have emerged as promising candidates for TCFs due to their superior electrical conductivity, high transmittance, and durability under bending stress [7,8]. The interconnected nanowire

networks facilitate electron flow, reducing sheet resistance and enabling flexibility. However, challenges remain, particularly in the synthesis and printing of AgNW-based inks.

The polyol process is the most common method for synthesizing AgNWs, which has also been extensively investigated and further optimized over the past years [9–11]. However, it is energy-intensive, requiring high temperatures (>150 °C), and relies on reagents such as ethylene glycol (EG) and polyvinylpyrrolidone (PVP), which are derived from fossil fuels. EG, in particular, poses environmental concerns due to its toxicity to aquatic life [12]. Furthermore, scaling up the polyol process is challenging and results in high production costs, raising questions about its economic feasibility.

Printing AgNW-based conductive patterns also presents difficulties. Achieving high-quality patterns, with sharp lines, high resolution, and minimal surface roughness requires careful optimization of ink rheology, including shear-thinning behavior and viscosity, as well as the composition of the ink, which typically includes binders, solvents, and nanostructured fillers.

Among the various printing methods, screen printing is widely used due to its simplicity, fine resolution, and scalability. The ink undergoes shear stress as it is forced through a mesh onto a substrate, with shear rates typically ranging from 0.1–200 1/s depending on mesh size and squeegee movement [13–17]. Rapid viscosity recovery after shear stress is crucial for maintaining sharp-edged lines [18,19]. While screen printing is versatile, it often results in significant material wastage. Inkjet printing, on the other hand, enables high-resolution patterning by depositing ink droplets tens of micrometers in diameter onto a substrate [20,21]. This method requires inks with low viscosity (1–30 cP) to prevent nozzle clogging [22,23]. However, the high aspect ratio of AgNWs can still pose clogging issues, often necessitating nanowire shortening via sonication [24]. The direct writing approach, a mechanized process typically involving 3D printing instrument, offers cost-effective and customizable printing solutions. It requires inks with intermediate viscosity to ensure smooth flow and shape retention after deposition [25]. Despite its advantages, direct writing is limited by its relatively low resolution and thicker pattern lines, which are unsuitable for miniaturized circuits.

In all printing processes, the timescale for viscosity recovery significantly influences line sharpness and film leveling [18]. The "Stretched Exponential" model [26,27] describes this transition (Equation (1)), where viscosity recovery is influenced by factors such as nanostructure content and aspect ratio. Studies have shown that higher AgNW content and aspect ratios improve viscosity recovery and printing performance.

$$\eta = \eta_0 + (\eta_\infty - \eta_0)(1 - \exp(-\frac{t}{\tau})^r) \quad (1)$$

where η is the viscosity at time t, η_0 is the viscosity at the high shear rate, η_∞ is the viscosity at the low shear rate, τ is the transition characteristic time, and r is a dimensionless constant, which is equal to one in most cases. The values for η_0 and η may be obtained using the peak hold test (applying a step increase to the shear rate followed by a decrease to the initial shear rate to mimic the ink charging sequence [28]).

Hemmati et al. [18] investigated the characteristic recovery time using the same equation (Equation (1)) by testing inks with different commercially available AgNW content. They found that the characteristic time decreased (reaching as low as 20.9 s) with an increase in the Ag nanostructure content (up to 6 wt.%). In another study, Liang et al. [19] also investigated the rheological behavior of the AgNW ink by measuring the viscosity recovery percentage after an applied shear stress, for different AgNW compositions. They showed that for a medium AgNW composition of 6.6 wt.%, a maximum viscosity recovery percentage of 59.4% can be obtained after 10 s of a step change in shear rate (from 200 to 0.1 1/s). After 50 s, the viscosity recovery percentage increased to 85.9%. However, for a higher content of AgNW (7.3 wt.%), 58.5% of the initial viscosity value was obtained. This behavior was attributed to the high viscosity of the ink at higher AgNW content [19,29].

For high-precision ink printing, three criteria are key: (1) The ink's viscosity should be suitable for smooth printing, avoiding droplet formation or nozzle blockage. (2) The ink should quickly recover its viscosity after extrusion to maintain shape. (3) Shrinkage during drying should be minimized using a high colloid volume, with high-aspect-ratio silver nanowires (AgNWs) to prevent nozzle clogging. [25,30–34].

AgNWs synthesized through the polyol process, initially developed in 2001, [9] have been widely used for the preparation of conductive ink. However, to the best of our knowledge, the large-scale green and sustainable synthesis of AgNWs and their applications in conductive ink preparation have not been extensively studied. To address the limitations of conventional synthesis methods, we previously developed a room-temperature process for synthesizing AgNWs using tannic acid as both a reducing and capping agent. This green and sustainable method eliminates the need for high temperatures and additional capping agents. However, the yield (~50%) and application of these AgNWs remain limited. This study builds upon our prior work, focusing on the large-scale, sustainable synthesis of AgNWs and their integration into conductive inks for advanced TCF manufacturing.

2. Methodology

2.1. Materials

Silver nitrate ($AgNO_3$, MW: 169.87 g/mol, product number: S0139), tannic acid ($C_{76}H_{52}O_{46}$, MW: 1701.2 g/mol, product number: 403040), nitric acid (HNO_3, 70% ACS reagent, MW: 63.01 g/mol, product number: 438073), and sodium carboxymethyl cellulose (CMC, MW~90,000 g/mol, product number: 419273) were purchased from Sigma Aldrich (St. Louis, MO, USA). Dispex ultra FA 4416 was purchased from BASF© (Florham Park, NJ, USA) as the dispersing agent and was used for conductive ink preparation. Deionized water (DIW, ASTM type II) was used as the solvent to prepare aqueous $AgNO_3$ and tannic acid solutions, as well as the conductive ink.

2.2. Synthesis and Isolation of AgNWs

For AgNWs synthesis with high throughput compared to our previously published study (5 mM tannic acid and $AgNO_3$ solutions), aqueous tannic acid and $AgNO_3$ solutions (both 20 mL, 100 mM each) were prepared. The pH of the tannic acid solution was adjusted to 1.25 by adding HNO_3. The tannic acid solution was then added to a 100 mL round glass flask, and the $AgNO_3$ solution was added dropwise. The reaction was continued at room temperature for 4 h. The flask was exposed to white fluorescent light at 676 LUX during the whole reaction because it assists the reduction process [35]. After the synthesis process was completed, the AgNWs suspension was centrifuged 4 times in DIW at 5000 rpm, with the supernatant being removed after each centrifugation step.

2.3. Scanning Electron Microscopy (SEM) Characterization

AgNWs were characterized by the FEI Quanta 600 (Stillwater, OK, USA) field-emission gun Environmental Scanning Electron Microscope at the Oklahoma State University microscopy laboratory. To do the characterization, 100 µL of the AgNWs suspension was pipetted onto smooth carbon tabs taped to aluminum pins. The samples were then kept at dry and room temperature conditions for 24 h to allow the samples to dry. The pins containing the AgNWs were then put on sample holders in the SEM instrument for characterization.

2.4. Conductive Ink Preparation

The AgNW-based conductive ink was prepared by mixing the AgNWs suspended in DIW, CMC, and the Dispex Ultra FA 4416 dispersing agent. The ink was prepared at different AgNWs weight percentages (2, 5, 10, and 20 wt.%), while the weight percentage of CMC and the dispersing agent were both kept at 6 wt.%. The combination of AgNWs and other nanostructures, aside from nanowires, was used for conductive ink preparation.

2.5. Rheological Tests

To investigate the rheological properties of the prepared conductive ink, the ink sample was analyzed using a TA Instrument's© Discovery HR-10 Rheometer (New Castle, DE, USA). To do so, a 25 mm geometry was used, and three main tests were performed including flow sweep, peak hold, and frequency sweep tests. After geometry definition and test setup, the ink sample was poured onto the sample holder disk (peltier plate) and trapped between the geometry and the disk. The trim gap (gap set for trimming the sample prior to the rheological test) was 1050 µm and the test gap (gap set for rheological testing) was 1000 µm. A 3-min soak time was allowed for the ink to reach the desired temperature.

2.6. Conductive Ink Printing Rheological Simulation

To simulate the ink printing process using screen printing, the peak hold test was performed using the rheometer. In the first step of the peak hold test, the ink was subjected to a low shear rate of 0.1 1/s for 40 s to simulate ink at rest. In the second step, the ink was subjected to a high shear rate of 400 1/s for 20 s to simulate ink under printing shear stress. In the third step, the shear rate was reduced back to 0.1 1/s for 100 s to simulate ink at resting condition after printing. To simulate the ink printing process using the direct writing method, a laboratory-made 3D printer (Figure 1) was considered as the model printer for the purpose of simulation, and its specifications were considered the direct printing simulation process. The 3D printer extruder operated based on a syringe and piston system. To initiate the printing process, the syringe would be loaded by conductive ink, with the ink being pushed manually by the piston to reach the printing needle tip. The syringe inner diameter was set at 12 mm, the main tube inner diameter was set at 3.5 mm, and the needle diameter was set 0.69 mm. To operate the

printer, the Repetier Host software can be used, which utilizes Gcode to define printing properties, such as the extruder movement rate, the flowrate, and the writing pattern.

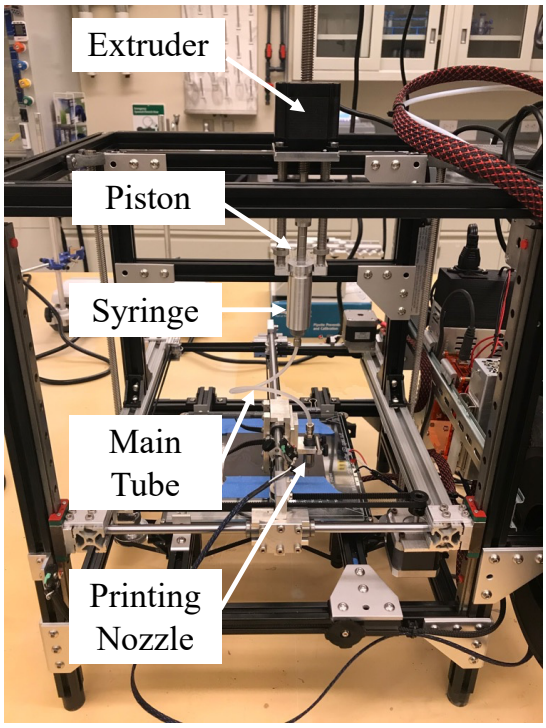

Figure 1. Laboratory-made 3D printer that its specifications were used for conductive inks printing process simulation.

3. Results and Discussion

3.1. Synthesis of AgNWs

We previously investigated the green synthesis of AgNWs using tannic acid and $AgNO_3$ at room temperature, as well as the effect of various factors such as light, Ag^+ ion and tannic acid concentration ratio, and pH [35,36]. In such cases, AgNWs were synthesized at moderate yield using both batch and continuous millifluidic processes (yield of 50 and 82%, respectively). We demonstrated that light is a significant factor in controlling the reduction rate of Ag^+ ions by tannic acid, and the fact that the reduction rate can be increased by increasing the pH and increasing the light intensity of UV-visible white fluorescent lamp. We also demonstrated that it is imperative that the ratio of tannic acid concentration to Ag^+ concentration is maintained at 1 to assist with the anisotropic growth of nanostructures that leads to the formation of nanowires [35]. The process by itself has several advantages, which are the minimal use of energy—due to the reaction being performed at room temperature—using a single-step process and just one reducing agent, which can also act as a capping and stabilizing agent, and using a sustainable and environmentally friendly reducing/capping agent, thereby decreasing chemical waste production. Despite all these advantages, the overall productivity of that process was limited and not feasible for preparation of conductive ink, which requires high silver nanostructure content, because $AgNO_3$ was used at a mere concentration of 5 mM. In the current study, we were able to produce AgNWs with an approximate yield of 90% using $AgNO_3$ and tannic acid at a much higher concentration (100 mM each) (Figure 2). This yield was higher compared to the yield acquired by both batch and millifluidic processes (~50 and 82%, respectively) previously synthesized at 5 mM of $AgNO_3$ and tannic acid. This was done by adjusting both the pH and light to control the reduction kinetics in a manner that leads to a controlled anisotropic growth process. Furthermore, acquiring such a high yield at lower concentrations was more difficult for two main reasons. The first issue is the increased sensitivity to experimental conditions. When the concentration is too low, the reaction can become highly sensitive to temperature, pH, and reducing agent/precursor concentration, which may ultimately lead to non-uniform morphologies and low yield. The second issue is the increased risk of contamination. When the concentration of the precursor (in this case, $AgNO_3$) is too low, the amount of impurities and contaminants in the reaction may be relatively large compared to concentration of Ag^+; therefore, interfering with the reaction in a disruptive manner. If favorable experimental parameters at high precursor/reducing agent concentration are discovered, such two challenges can be minimized. The reduction rate increases with an increase in the concentration of Ag^+ ions. However, reducing the pH to a

highly acidic value of 1.25 significantly decreases the reduction rate, offsetting the increase caused by the high Ag^+ concentration. Deviating from a pH of 1.25, either lower or higher, results in a reduced yield of AgNWs.

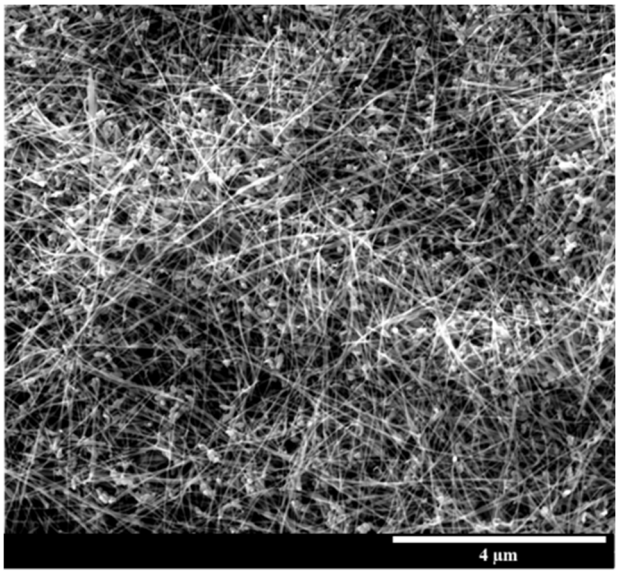

Figure 2. SEM image of silver nanowires (AgNWs) synthesized by tannic acid at room temperature. Average nanowire diameter: 32.9 ± 8.2 nm. Average nanowire length: 9.8 ± 4.1 µm.

3.2. Economic Analysis

To assess the economic feasibility of the tannic acid-mediated and polyol processes, the costs of the metal precursor ($AgNO_3$), reducing agent (tannic acid/ethylene glycol), capping agent (polyvinylpyrrolidone (PVP)), and electricity consumption by the hotplate were considered. To determine the cost of materials needed for a typical polyol process, a previous reference [37] was studied and the amounts of materials used in grams were initially documented. Then the cost per gram of materials were collected from the Sigma Aldrich website based on the product number associated with each material, considering the largest volumes available because it would be the most likely scenario for large-scale operations. For electricity consumption, the hotplates were assumed to have a range of power consumption from 300–1500 Watts, with the cost of electricity in the industry sector standing at 8.21 cents per KWh by the end of October 2024 according to the U.S Energy Information Administration (EIA) [38]. As a result, the minimum and maximum power consumption costs were calculated, and the average was used. In the case of a room-temperature process, such as the tannic acid-mediated synthesis, it would not be realistic to account for the total power consumption of the hotplate, because only magnetic stirring is active, which is estimated to account for about 5% of the total power consumption, nearly negligible compared to the power consumed by heating. However, the light usage should be considered for the tannic acid-mediated process because it relies on UV-Visible illumination by white fluorescent lamps which are 25 W strong.

To calculate the total grams of AgNWs synthesized in a typical polyol process, the amount of Ag^+ ions at the end of the reaction (performed according to Hemmati et al.'s [37] publication) was identified using a spectrophotometric technique we used in one of our previous publications [35]; which was followed by the calculation of the Ag^0 produced in the process as shown in Equation (2).

$$Ag^0(g)\ produced = initial\ Ag^+(g) - final\ Ag^+(g) \quad (2)$$

where the initial Ag^+ is known and the final Ag^+ is calculated by the spectrophotometric identification technique. The same technique was used to calculate the amount of Ag^0 produced by the tannic acid process. The conversion rate ($Ag^0\ produced/initial\ Ag^+ \times 100\%$) calculated based on the data from Equation (2) stands at 83.64% for the polyol process and 32.12% for the tannic acid- mediated process. Based on the materials and energy consumption costs, the production cost per gram of AgNWs can be calculated. For the tannic acid-mediated synthesis process, a correction factor of 10/9 (100%/90%) is considered due to its yield standing at 90%. Since this value is typically 99% or higher for the polyol process, it was neglected. Table 1 compares production cost per gram of AgNWs for the polyol process and the tannic acid-mediated process. The production cost is broken down into materials and electricity consumption costs for each process. The sum of these costs is then converted to $/g of AgNWs, taking into account the yield and conversion rates of each process. For brevity, only the electricity, materials, and total production costs, and grams of AgNWs produced per process are included. Reader

can refer to the supplemental Excel file for more information and to see how these conversions are specifically made.

Table 1. Comparison of the production costs ($/grams of AgNWs) between polyol process and the tannic acid-mediated process.

Method	Energy (Electricity) Consumption Cost per Process ($)	Materials Cost per Process ($)	Grams of AgNWs Produced per Process	Production Cost $/g of AgNWs
Our method (tannic acid-mediated synthesis)	0.02	2.18	0.0689	35.59
Hemmati et al. [37] (2017)	0.11	1.88	0.0382	52.12

As demonstrated in Table 1, the production cost per gram of AgNWs is lower in the tannic acid-mediated synthesis compared to the conventional polyol process. Although the production cost depends on the very specifics of a synthesis process, it can be reduced 31.72% by using the tannic acid-mediated process. Despite having a lower conversion rate of the tannic acid-mediated synthesis process compared to the polyol process, the tannic acid-mediated process is much cheaper and is environmentally friendly, making its industrial applications simpler and more feasible compared to the conventional polyol process.

3.3. Rheological Analysis

When investigating the rheological behavior of a printable nanostructure-based conductive ink, 6 main factors should be considered, including viscosity, shear rate, weight percentage and morphology of the nanostructures, solvent, temperature, and more importantly the printing conditions [25,28,39–42]. The first three were discussed in the introduction section. The effect of solvent is also important because solvents with higher surface tension tend to increase the viscosity of the ink. Temperature is another important factor because higher temperatures can reduce the viscosity of the conductive ink while lower temperatures can increase it. This characteristic can be beneficial in the printing process as it allows for fine-tuning the rheological behavior of the ink to match the requirements of the printing process by temperature adjustments. Lastly, for the sake of proper rheological measurements, the specific printing condition needs to be considered. Printing conditions such as printing speed, ink flowrate, width/diameter of printing nozzle, and width/diameter of flow channel can affect the rheological behavior of the ink during the printing process. Based on previous tests with our laboratory-made printer, the overall viscosity of the ink (at rest) should be more than 5 Pa.s. Lower viscosities may result in nozzle drip, which leads to an inconsistent printed pattern. Higher viscosities can be used; however, this depends on the colloidal content and the concentration of the binder. One should note that there is no defined viscosity range for printing applications, and the required viscosity and shear rate is application specific.

3.3.1. Rheological Behavior of AgNW-Based Conductive Ink and the Effect of Silver (Ag) Nanostructure Content

Flow Sweep Test

To investigate the rheological behavior of the ink, the first test was the flow sweep test. This test shows the overall viscosity of the ink change with respect to shear rates and determines whether the ink has shear-thinning or shear-thickening behavior. A conductive ink that is used for screen printing or direct printing applications should have a shear thinning characteristic. Figure 3 shows the viscosity of the ink vs. shear rate for concentration of 2, 5, 10, and 20 wt.% of Ag nanostructures at room temperature (25 °C). As demonstrated, for all Ag nanostructure contents, the viscosity of the ink decreases with increase in shear rate, indicating the shear-thinning behavior of the ink. However, the decline in viscosity is more pronounced for the ink with higher Ag nanostructure content, whereas it is less pronounced for the ink with lower silver nanostructure content.

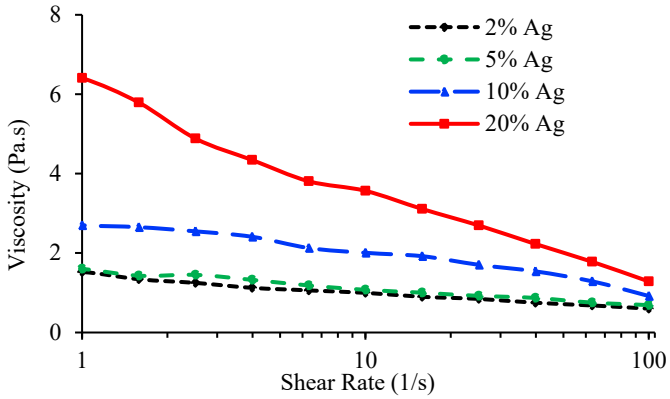

Figure 3. Flow sweep test for conductive ink with different silver nanostructure contents.

Frequency Sweep Test

The frequency sweep test was performed to analyze the viscoelastic behavior of the ink, and to extract valuable information about the effect of colloidal forces and the interaction of nanostructures. Two main variables are provided by the frequency sweep test including storage modulus and loss modulus. The storage modulus (G′) is a measure of the elastic behavior of the ink while the loss modulus (G″) is a measure of the viscous behavior of the ink. Figure 4 shows the frequency sweep test results, demonstrating storage and loss modulus vs. angular frequency for different Ag nanostructure contents at room temperature (25 °C). Both loss and storage modulus increase with increasing the Ag nanostructure content. This means that the resistance of the ink to deformation increases as the Ag nanostructure content increases. However, for all Ag nanostructure contents, and for the whole angular frequency spectrum, the loss modulus is more than the storage modulus, meaning that the viscous effect is dominant compared to the elastic effect. A more detailed analysis of the viscous/elastic effect can be provided by describing the tan delta variable (tan δ) as shown in Equation (3).

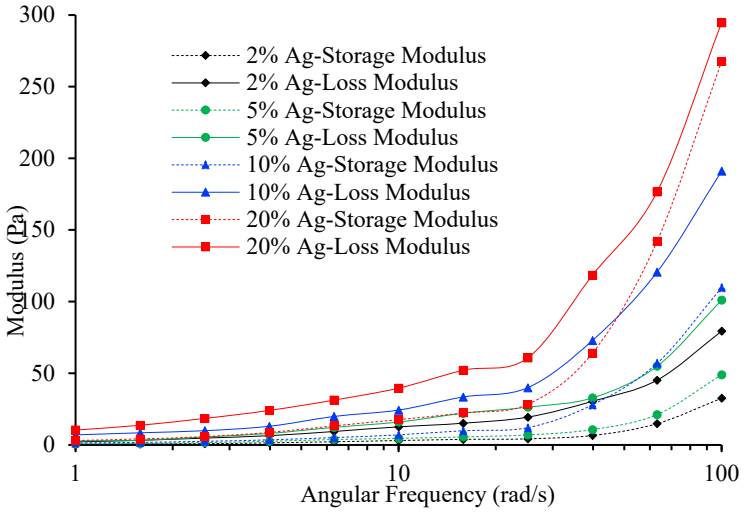

Figure 4. Frequency sweep test for conductive ink with different silver nanostructure contents.

$$tan\delta = \frac{G''}{G'} \tag{3}$$

where G″ (Pa) is the loss modulus and G′ (Pa) is the storage modulus. Thus, a higher tan δ accounts for a stronger viscous behavior while a lower tan δ accounts for a stronger elastic behavior. Figure 5A shows tan δ vs. angular frequency for different Ag nanostructure contents. As demonstrated, tan δ decreases overall for all Ag nanostructure contents, meaning that the elastic effects become stronger at higher frequencies. This is because at lower frequencies, nanostructures have more time to move within the binder matrix, which can result in a more viscous response, while at higher frequencies, nanostructures have less time to move within binder matrix due to

the high oscillation factor, which ultimately results in a more elastic response. The more the Ag nanostructure content, the lower the tan δ at high frequencies, meaning that the elastic response becomes stronger as the Ag nanostructure content increases.

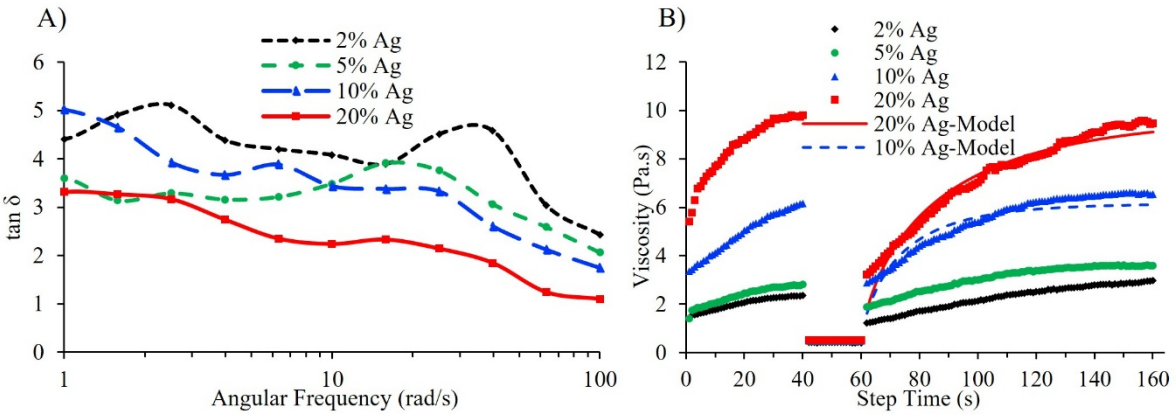

Figure 5. (**A**) tan δ (ratio of viscous modulus to elastic modulus) for conductive ink with different silver nanostructure contents. (**B**) Peak hold test for conductive ink with different silver nanostructure contents (high shear rate= 400 1/s and low shear rate= 0.1 1/s).

Nevertheless, for all Ag nanostructure contents and for the whole angular frequency spectrum, tan δ is higher than one, meaning that the viscous response is still dominant compared to the elastic response even for the highest angular frequencies. There is a "cross-over frequency" where the value of G′ equalizes G″, and tan δ becomes equal to 1. After this frequency, the elastic response will be more dominant rather than the viscous response. However, this frequency was not reached in the range of angular frequency used in this study.

Peak Hold Test: High-Shear Rate Printing

In the peak hold test, the ink is first subjected to a low shear rate, simulating ink at rest, and then subjected to a high shear rate, simulating ink under increased stress during printing, and then back to the low shear rate, simulating ink at rest or recovery after printing. This test is very useful for printing applications such as screen printing, inkjet printing, and direct writing or 3D printing because it can simulate the flow of the ink during the printing process, and therefore determines whether the ink is suitable for such applications. The peak hold test was performed for the inks with Ag nanostructures content of 2, 5, 10, and 20 wt.%. The sample was first subjected to low shear rate at 0.1 1/s for 40 s, followed by high shear rate at 400 1/s for 20 s, and then back to 0.1 1/s for 100 s. Figure 5B shows the peak hold test results for different Ag nanostructure contents at room temperature (25 °C). As demonstrated, the overall viscosity of the ink increases as the Ag nanostructure content is increased. However, it takes longer for the higher Ag nanostructure content ink to retain its original viscosity. By using the build-up structure model (Equation (1)), the characteristic time for transition can be identified. Table 2 shows the characteristic times of transition for Ag nanostructure contents of 10 and 20 wt.%. The characteristic time for transition in the case of 20 wt.% Ag nanostructure content is almost twice of that of 10 wt.% Ag nanostructure content, which explains the longer time for viscosity retention. For 2 and 5 wt.% of Ag nanostructure contents, the structure build-up model did not provide a statistically significant R^2 value, and therefore could not fit the data. One possible reason for this may be the high shear rate; because high shear rates—particularly for low colloidal content—can cause structural deformation in the ink, which causes the experimental data to deviate from the structure build-up model. Nevertheless, in both 2, and 5 wt.% Ag nanostructure contents, the viscosity retains its original value (viscosity just before being subjected to the higher shear rate) in less than 60 s compared to 100 s for the 20 wt.% Ag nanostructure content. We used the 400 1/s shear rate, as a significantly high shear rate value to observe the thixotropic behavior of the ink at very high shear. The relatively long transition time caused by the 400 1/s shear rate suggests that this value may not be a proper shear rate in the printing process. When the shear rate increases, it also makes it harder for the ink to retain its original structure. Therefore, in this case, a lower shear rate is required to allow for a rapid transition.

Table 2. Stretched Exponential model parameters from the structure build-up model for 10 and 20 wt.% silver nanostructure contents.

Ag nanostructure content	10%	20%
Characteristic time τ (s)	13.75	27.04
r (dimensionless constant)	0.78	0.73
R^2	0.91	0.97

3.3.2. Effect of Temperature

Flow Sweep Test

The flow sweep test was repeated at 30 and 40 °C to observe the change in viscosity and shear-thinning behavior of the ink with respect to temperature. The frequency sweep, and the peak hold tests were done for the 20 wt.% Ag nanostructure content because 20 wt.% Ag nanostructure content was the most favorable condition for the direct writing application. Figure 6A shows the viscosity with respect to shear rate at 25, 30, and 40 °C. The curve for 25 °C is the Same provided in Figure 3. As demonstrated, the viscosity decreases by increasing the temperature. The decline in viscosity with respect to increasing shear rate is more rapid at lower temperatures; this behavior is similar to that of lower Ag nanostructure content ink.

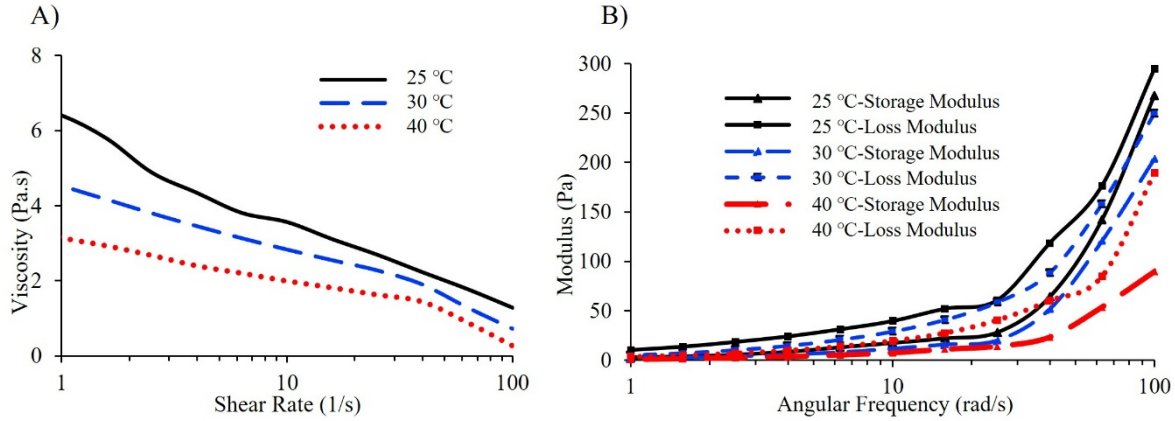

Figure 6. (**A**) Flow sweep test for conductive ink with 20 wt.% silver nanostructure content at different temperatures. (**B**) Frequency sweep test for conductive ink with 20 wt.% silver nanostructure content at different temperatures.

Frequency Sweep Test

The frequency sweep test was performed at 30 and 40 °C to observe the viscoelastic behavior of the ink. Figure 6B shows the storage and loss modulus of the ink with respect to angular frequency for different temperatures. As shown, both storage and loss modulus decrease as the temperature increases. With increasing temperature, overall resistance of the ink to deformation decreases. This is an important phenomenon and should be considered for printing processes at other temperatures than that of room temperature. To analyze the dominance of either the storage or loss modulus, tan δ with respect to angular frequency for all temperatures should be considered, and Figure 7A shows this comparison. As demonstrated, for all temperatures, tan δ decreases by increasing angular frequency, which means that the elastic response becomes more dominant at higher frequencies. However, there is a noticeable difference between the curves. After the frequency of approximately 4 rad/s, tan δ for inks at 30 and 40 °C surpasses the one at room temperature, meaning that at low frequencies, the viscous response is more dominant in the case of lower temperatures, while at higher frequencies, the elastic response is more dominant. This phenomenon occurs because at higher temperatures, the nanostructures can move slightly easier, and therefore allows the ink to maintain its viscous response.

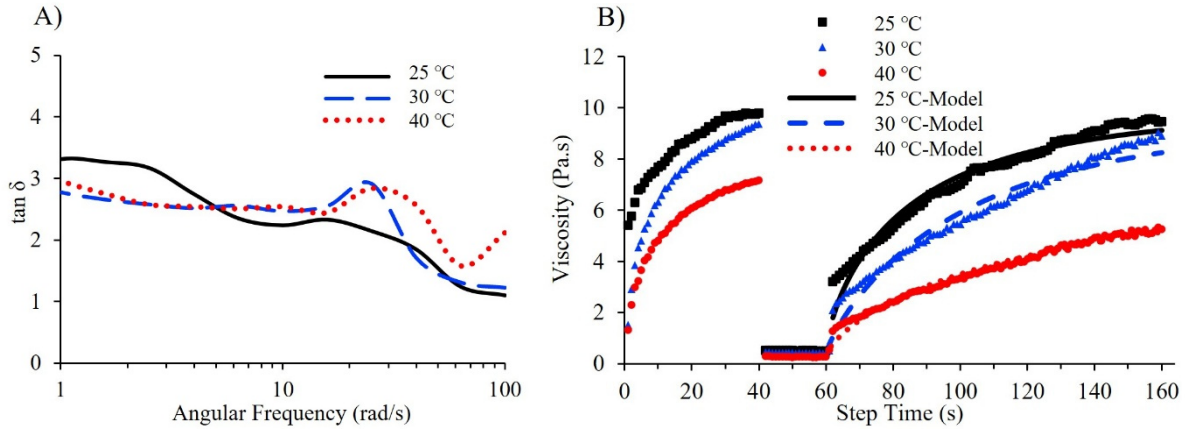

Figure 7. (**A**) Tan δ (ratio of viscous modulus to elastic modulus) for conductive ink with 20 wt.% silver nanostructure content at different temperatures. (**B**) Peak hold test for conductive ink with 20 wt.% silver nanostructure content at different temperatures (high shear rate = 400 1/s and low shear rate = 0.1 1/s).

Peak Hold Test: High-Shear Rate Printing

Similar to the peak hold test performed for different Ag nanostructure contents at room temperature, the peak hold test was performed to observe the shear thinning thixotropic behavior of the ink at different temperatures. Figure 7B shows the peak hold test results for the viscosity sketched with respect to time at different temperatures. In all cases, the ink experiences a relatively high transition time to retain its original viscosity. To compare the characteristic times for transition, the build-up structure model was used to fit the data for three temperatures. Table 3 shows the model parameters for all temperatures.

Table 3. Stretched Exponential model parameters from the structure build-up model for different temperatures.

Temperature	25 °C	30 °C	40 °C
Characteristic time τ (s)	27.04	42.37	75.72
r (dimensionless constant)	0.73	0.86	0.73
R^2	0.97	0.96	0.98

3.3.3. Printing Simulation: Low-Shear Rate Printing

To simulate the printing process, the situation that the ink undergoes inside the printer needs to be analyzed in detail. In a syringe-piston system, where the ink is squeezed through a cylindrical tube, the shear rate for a shear-thinning material can be calculated by the Rabinowitsch-Mooney correction relation as shown in Equation (4) [43].

$$\dot{\gamma}_w = \frac{Q}{\pi r^3}[3 + \frac{1}{n}] \quad (4)$$

where Q is the flowrate inside the tube (mm^3/s), r is the tube radius (mm), $\dot{\gamma}_w$ is the shear rate at the wall of the tube (1/s), and n is the dimensionless power law index, which will be derived from the power-law as shown in Equation (5).

$$\sigma = k\dot{\gamma}^n \quad (5)$$

where σ is the shear stress (pa), $\dot{\gamma}$ is the shear rate (1/s), k is the consistency index (pa.s), and n is the power-law index. The power-law equation relates shear rate and shear stress for a non-Newtonian fluid. In the case of $n = 1$, the fluid is Newtonian, in the case of $n > 1$, the fluid has a shear-thickening behavior, and in the case of $n < 1$, the fluid has a shear-thinning behavior. The rheometer was used to simulate the printing process by performing the peak hold test on the AgNW-based ink, with 20 wt.% Ag nanostructure content. To do so, n should be calculated by fitting the power-law equation (Equation (5)) with the experimental data. Figure 8A shows shear stress vs. shear rate for the experimental data (obtained by flow sweep test with the rheometer) and the fitted model. After calculating n, Equation (4) was used to calculate the shear rate inside the main tube of the printer. With n being equal to 0.58, the shear rate was 22.24 1/s inside the main tube. After the shear rate is calculated, the peak hold test can be performed using the calculated shear rate value. It was assumed that the printing process has already reached a steady state. It was also assumed that the shear rate within the nozzle and tube fittings can be neglected compared to the shear rate within the main tube. This assumption was made because the time the ink is

under shear stress inside the nozzle and tube fittings is a fraction of a second, and therefore negligible compared to 34.53 s in the main tube. Therefore, a consistent shear rate of 22.24 1/s was used for the high-shear rate step in the peak hold test, which lasted for 34.53 s. The low shear rate, simulating the ink at rest, was considered as 0.1 1/s. The first low-shear rate step lasted for 40 s, and the second low-shear rate step lasted for 100 s. The test was done at room temperature as the printing process is also performed at room temperature. Figure 8B shows the peak hold test performed for the ink with 20 wt.% silver nanostructure content. As demonstrated, after undergoing stress at 22.24 1/s for 34.53 s, the ink follows smooth transition back to its original viscosity. The structure build-up model was used to fit the experimental data after high shear rate removal. The characteristic time for transition in this case was equal to 1.78 s, which is significantly lower compared to the one previously calculated for 20 wt.%-Ag nanostructure-content ink, undergoing 400 1/s shear rate. This suggests that the low shear rate of 22.24 1/s allows for a rapid and smooth transition during the ink printing process.

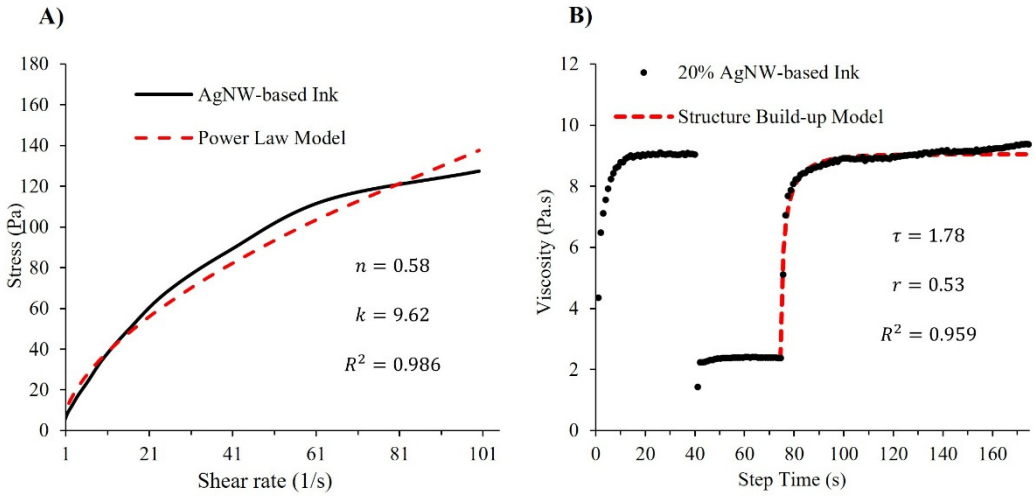

Figure 8. (**A**) Shear stress vs. shear rate, and the fitted power-law model for the tannic acid-synthesized AgNWs-based conductive ink (result obtained by the flow sweep test). Ag nanostructure content: 20 wt.%. (**B**) Peak hold test for tannic acid-synthesized AgNWs-based conductive ink with Ag nanostructure content of 20 wt.% (high shear rate = 22.24 1/s and low shear rate = 0.1 1/s).

4. Conclusions

This study presents a high-yield (90%), environmentally friendly, and cost-effective method for synthesizing AgNWs at room temperature. The synthesis process involved the use of tannic acid and silver nitrate, with the reaction being moderated by UV-visible light emission. Additionally, the approach demonstrated sustainability as a key feature. It was demonstrated that the production cost per gram of AgNWs can be decreased by at least 31.72% compared to the polyol process. Such a reduction in cost greatly enables the utilization of AgNWs in the realm of large-scale conductive ink manufacturing. The use of white fluorescent light for small-scale synthesis of AgNWs may face challenges when scaled up due to varying light intensity and distribution. Future work could focus on optimizing light delivery in larger reactors to ensure consistent reaction conditions. Furthermore, the rheological behavior of AgNW-based conductive ink for printing applications was investigated by performing rheological tests at different contents of silver nanostructure and temperatures. The conductive ink demonstrated a shear-thinning thixotropic behavior for all silver nanostructure contents (2, 5, 10, and 20 wt.%), and all temperatures (25, 30, and 40 °C). Three general rheological tests were performed, namely, the flow sweep, frequency sweep, and peak hold tests. The flow sweep test revealed the shear-thinning behavior of the ink, indicating a decrease in viscosity with increasing shear rates. This decline in viscosity was more pronounced for higher silver nanostructure contents and lower temperatures. The frequency sweep test illustrated the viscoelastic behavior of the ink and its overall resistance to deformation. The results demonstrated that higher silver nanostructure contents led to increased storage and loss modulus in the ink, resulting in greater resistance to deformation. It was demonstrated that, in general, the viscous response dominates over the elastic response, regardless of the silver nanostructure content and temperature. However, with higher silver nanostructure contents, the elastic response becomes more pronounced, particularly with increasing oscillation frequency. Additionally, at 25 °C, the ink exhibits a stronger viscous response at lower oscillation frequencies compared to the behavior observed at 30 and 40 °C. At higher oscillation frequencies, the elastic response was more dominant for the ink at 25 °C compared to 30 and 40 °C.

The peak hold tests indicated that the time for viscosity and shape retention after exposure to high shear rate (400 1/s) was longer for ink samples with higher silver nanostructure contents and higher temperatures. Finally, to simulate the direct writing process, a peak hold test was conducted on the environmentally friendly AgNW-based ink using a custom laboratory printer. The ink exhibited a smooth transition in retaining its structure after being subjected to the shear rate of 22.24 1/s during printing process. This transition occurred much more rapidly when using the direct writing procedure compared to the ink subjected to a high shear rate of 400 1/s. This indicates that direct writing is better suited for printing the ink with low colloidal content due to its lower shear rate, whereas screen printing is more favorable for printing high-content and high-viscosity ink due to its utilization of high shear rates. In conclusion, the cost-effective synthesis of AgNWs proves to be extremely valuable for large-scale production of conductive ink. This is supported by both the economic analysis and the rheological tests conducted on the prepared conductive ink.

Supplementary Materials: The supporting information can be downloaded at: https://www.sciltp.com/journals/mi/2025/1/615/s1.

Author Contributions: S.K.: Writing the original draft, conducting investigations, developing methodologies, collecting data, and creating visualizations; F.N.: Analyzing data, generating graphs, and editing; S.H.: Managing the project, acquiring funding, supervising, reviewing, revising, and editing.

Funding: This work was supported by startup funds from the College of Engineering, Architecture, and Technology (CEAT) at Oklahoma State University as well as startup funds from the College of Art and Science at the University of Southern Mississippi.

Data Availability Statement: The relevant data supporting the findings of this study are included in the manuscript and supplementary materials. Additional datasets generated and/or analyzed during this study are available from the corresponding author upon reasonable request.

Acknowledgement: We would like to acknowledge our colleague at Oklahoma State University, James Smay (Professor and Head, School of Materials Science and Engineering), for designing, providing, and training the students on the 3D printer used in this manuscript.

Conflicts of Interest: The authors declare no conflict of interest.

References

1. Hasan, M.M.; Hossain, M.M. Nanomaterials-patterned flexible electrodes for wearable health monitoring: A review. *J. Mater. Sci.* **2021**, *56*, 14900–14942. https://doi.org/10.1007/s10853-021-06248-8.
2. Manjakkal, L.; Núñez, C.G.; Dang, W.; Dahiya, R. Flexible self-charging supercapacitor based on graphene-Ag-3D graphene foam electrodes. *Nano Energy* **2018**, *51*, 604–612. https://doi.org/10.1016/j.nanoen.2018.06.072.
3. Lin, C.H.; Fu, H.C.; Cheng, B.; Tsai, M.L.; Luo, W.; Zhou, L.; Jang, S.H.; Hu, L.; He, J.H. A flexible solar-blind 2D boron nitride nanopaper-based photodetector with high thermal resistance. *NPJ 2D Mater. Appl.* **2018**, *2*, 23. https://doi.org/10.1038/s41699-018-0070-6.
4. Tseberlidis, G.; Trifiletti, V.; Le Donne, A.; Frioni, L.; Acciarri, M.; Binetti, S. Kesterite solar-cells by drop-casting of inorganic sol–gel inks. *Sol. Energy* **2020**, *208*, 532–538. https://doi.org/10.1016/j.solener.2020.07.093.
5. Lee, S.; Jang, J.; Park, T.; Park, Y.M.; Park, J.S.; Kim, Y.K.; Lee, H.K.; Jeon, E.C.; Lee, D.K.; Ahn, B.; et al. Electrodeposited silver nanowire transparent conducting electrodes for thin-film solar cells. *ACS Appl. Mater. Interfaces* **2020**, *12*, 6169–6175. https://doi.org/10.1021/acsami.9b17168.
6. Gonzalez-Garcia, L.; Maurer, J.H.M.; Reiser, B.; Kanelidis, I.; Kraus, T. Ultrathin gold nanowires for transparent electronics: Breaking barriers. *Procedia Eng.* **2016**, *141*, 152–156. https://doi.org/10.1016/j.proeng.2015.08.1120.
7. Yang, X.; Du, D.; Wang, Y.; Zhao, Y. Silver nanowires inks for flexible circuit on photographic paper substrate. *Micromachines* **2018**, *10*, 22. https://doi.org/10.3390/mi10010022.
8. Yang, L.; Xu, X.; Yuan, Y.; Li, Z.; He, S. Meter-scale transparent conductive circuits based on silver nanowire networks for rigid and flexible transparent light-emitting diode screens. *Opt. Mater. Express* **2019**, *9*, 4483–4496. https://doi.org/10.1364/OME.9.004483.
9. Sun, Y.; Gates, B.; Mayers, B.; Xia, Y. Crystalline silver nanowires by soft solution processing. *Nano Lett.* **2002**, *2*, 165–168. https://pubs.acs.org/doi/10.1021/nl010093y.
10. Parente, M.; Van Helvert, M.; Hamans, R.F.; Verbroekken, R.; Sinha, R.; Bieberle-Hütter, A.; Baldi, A. Simple and fast high-yield synthesis of silver nanowires. *Nano Lett.* **2020**, *20*, 5759–5764. https://doi.org/10.1021/acs.nanolett.0c01565.
11. Shi, Y.; He, L.; Deng, Q.; Liu, Q.; Li, L.; Wang, W.; Xin, Z.; Liu, R. Synthesis and applications of silver nanowires for transparent conductive films. *Micromachines* **2019**, *10*, 330. https://doi.org/10.3390/mi10050330.
12. Staples, C.A.; Williams, J.B.; Craig, G.R.; Roberts, K.M. Fate, effects and potential environmental risks of ethylene glycol: A review. *Chemosphere* **2001**, *43*, 377–383. https://doi.org/10.1016/S0045-6535(00)00148-X.

13. Zeng, P.; Tian, B.; Tian, Q.; Yao, W.; Li, M.; Wang, H.; Feng, Y.; Liu, L.; Wu, W. Screen-printed, low-cost, and patterned flexible heater based on Ag fractal dendrites for human wearable application. *Adv. Mater. Technol.* **2019**, *4*, 1800453. https://doi.org/10.1002/admt.201800453.
14. Faddoul, R.; Reverdy-Bruas, N.; Blayo, A. Formulation and screen printing of water based conductive flake silver pastes onto green ceramic tapes for electronic applications. *Mater. Sci. Eng. B Solid-State Mater. Adv. Technol.* **2012**, *177*, 1053–1066. https://doi.org/10.1016/j.mseb.2012.05.015.
15. Ke, S.H.; Xue, Q.W.; Pang, C.Y.; Guo, P.W.; Yao, W.J.; Zhu, H.P.; Wu, W. Printing the ultra-long Ag nanowires inks onto the flexible textile substrate for stretchable electronics. *Nanomaterials* **2019**, *9*, 686. https://doi.org/10.3390/infrastructures4020020.
16. Li, W.; Yang, S.; Shamim, A. Screen printing of silver nanowires: Balancing conductivity with transparency while maintaining flexibility and stretchability. *NPJ Flex. Electron.* **2019**, *3*, 13. https://doi.org/10.1038/s41528-019-0057-1.
17. He, X.; Shen, G.; Xu, R.; Yang, W.; Zhang, C.; Liu, Z.; Chen, B.; Liu, J.; Song, M. Hexagonal and square patterned silver nanowires/PEDOT composite grids by screen printing for uniformly transparent heaters. *Polymers* **2019**, *11*, 468. https://doi.org/10.3390/polym11030468.
18. Hemmati, S.; Barkey, D.P.; Gupta, N. Rheological behavior of silver nanowire conductive inks during screen printing. *J. Nanoparticle Res.* **2016**, *18*, 249. https://doi.org/10.1007/s11051-016-3561-4.
19. Liang, J.; Tong, K.; Pei, Q. A water-based silver-nanowire screen-print ink for the fabrication of stretchable conductors and wearable thin-film transistors. *Adv. Mater.* **2016**, *28*, 5986–5996. https://doi.org/10.1002/adma.201600772.
20. Patil, P.; Patil, S.; Kate, P.; Kulkarni, A.A. Inkjet printing of silver nanowires on flexible surfaces and methodologies to improve the conductivity and stability of the printed patterns. *Nanoscale Adv.* **2021**, *3*, 240–248. https://doi.org/10.1039/d0na00684j.
21. Huang, Q.; Al-Milaji, K.N.; Zhao, H. Inkjet printing of silver nanowires for stretchable heaters. *ACS Appl. Nano Mater.* **2018**, *1*, 4528–4536. https://doi.org/10.1021/acsanm.8b00830.
22. Lee, H.H.; Chou, K.S.; Huang, K.C. Inkjet printing of nanosized silver colloids. *Nanotechnology* **2005**, *16*, 2436–2441. https://doi.org/10.1088/0957-4484/16/10/074.
23. Liu, Z.; Su, Y.; Varahramyan, K. Inkjet-printed silver conductors using silver nitrate ink and their electrical contacts with conducting polymers. *Thin Solid Films* **2005**, *478*, 275–279. https://doi.org/10.1016/j.tsf.2004.11.077.
24. Finn, D.J.; Lotya, M.; Coleman, J.N. Inkjet printing of silver nanowire networks. *ACS Appl. Mater. Interfaces* **2015**, *7*, 9254–9261. https://doi.org/10.1021/acsami.5b01875.
25. Kuzmenko, V.; Karabulut, E.; Pernevik, E.; Enoksson, P.; Gatenholm, P. Tailor-made conductive inks from cellulose nanofibrils for 3D printing of neural guidelines. *Carbohydr. Polym.* **2018**, *189*, 22–30. https://doi.org/10.1016/j.carbpol.2018.01.097.
26. Barnes, H.A. Thixotropy—A review. *J. Nonnewton Fluid Mech.* **1997**, *70*, 1–33. https://doi.org/10.1016/S0377-0257(97)00004-9.
27. Mallik, S. Study of the Time-Dependent Rheological Behaviour of Lead-Free Solder Pastes and Flux Mediums Used for Flip-Chip Assembly Applications. Ph.D. Thesis, University of Greenwich, London, UK, 2009.
28. Hemmati, S.; Barkey, D.P.; Gupta, N.; Banfield, R. Synthesis and characterization of silver nanowire suspensions for printable conductive media. *ECS J. Solid State Sci. Technol.* **2015**, *4*, 3075–3079. https://doi.org/10.1149/2.0121504jss.
29. Rudež, R.; Pavlič, J.; Bernik, S. Preparation and influence of highly concentrated screen-printing inks on the development and characteristics of thick-film varistors. *J. Eur. Ceram Soc.* **2015**, *35*, 3013–3023. https://doi.org/10.1016/j.jeurceramsoc.2015.04.035.
30. Smay, J.E.; Gratson, G.M.; Shepherd, R.F.; Cesarano, J.; Lewis, J.A. Directed colloidal assembly of 3D periodic structures. *Adv. Mater.* **2002**, *14*, 1279–1283. https://doi.org/10.1002/1521-4095(20020916)14:18<1279::AID-ADMA1279>3.0.CO;2-A.
31. Nair, N.M.; Daniel, K.; Vadali, S.C.; Ray, D.; Swaminathan, P. Direct writing of silver nanowire-based ink for flexible transparent capacitive touch pad. *Flex. Print. Electron.* **2019**, *4*, 045001. https://doi.org/10.1088/2058-8585/ab4b04.
32. Martin, G.D.; Hoath, S.D.; Hutchings, I.M. Inkjet printing—The physics of manipulating liquid jets and drops. *J. Phys. Conf. Ser.* **2008**, *105*, 012001. https://doi.org/10.1088/1742-6596/105/1/012001.
33. Yan, P.; Brown, E.; Su, Q.; Li, J.; Wang, J.; Xu, C.; Zhou, C.; Lin, D. 3D Printing Hierarchical Silver Nanowire Aerogel with Highly Compressive Resilience and Tensile Elongation through Tunable Poisson's Ratio. *Small* **2017**, *13*, 1701756. https://doi.org/10.1002/smll.201701756.
34. Compton, B.G.; Lewis, J.A. 3D-printing of lightweight cellular composites. *Adv. Mater.* **2014**, *26*, 5930–5935. https://doi.org/10.1002/adma.201401804.
35. Kaabipour, S.; Hemmati, S. Green, sustainable, and room-temperature synthesis of silver nanowires using tannic acid—Kinetic and parametric study. *Colloids Surfaces A Physicochem. Eng. Asp.* **2022**, *641*, 128495. https://doi.org/10.1016/j.colsurfa.2022.128495.
36. Kaabipour, S.; Hemmati, S. Continuous, green, and room-temperature synthesis of silver nanowires in a helically-coiled millifluidic reactor. *Colloids Surfaces A Physicochem. Eng. Asp.* **2023**, *659*, 130806. https://doi.org/10.1016/j.colsurfa.2022.130806.

37. Hemmati, S.; Barkey, D.P. Parametric study, sensitivity analysis, and optimization of polyol synthesis of silver nanowires. *ECS J. Solid State Sci. Technol.* **2017**, *6*, 132–137. https://doi.org/10.1149/2.0141704jss.
38. U.S Energy Information Administration (2024). Available online: https://www.eia.gov/electricity/monthly/epm_table_grapher.php?t=epmt_5_6_a (accessed on 5 January 2025).
39. Hong, H.; Jiyong, H.; Moon, K.S.; Yan, X.; Wong, C.P. Rheological properties and screen printability of UV curable conductive ink for flexible and washable E-textiles. *J. Mater. Sci. Technol.* **2021**, *67*, 145–155. https://doi.org/10.1016/j.jmst.2020.06.033.
40. Dzisah, P.; Ravindra, N.M. Modeling of Rheological Properties of Metal Nanoparticle Conductive Inks for Printed Electronics. In *TMS 2021 150th Annual Meeting & Exhibition Supplemental Proceedings*; Springer International Publishing: Berlin/Heidelberg, Germany, 2021; pp. 964–979. https://doi.org/10.1007/978-3-030-65261-6_86.
41. Yoon, I.S.; Oh, Y.; Kim, S.H.; Choi, J.; Hwang, Y.; Ju, B.K. 3D Printing of Self-Wiring Conductive Ink with High Stretchability and Stackability for Customized Wearable Devices. *Adv. Mater. Technol.* **2019**, *4*, 1900363. https://doi.org/10.1002/admt.201900363.
42. Hatala, M.; Gemeiner, P.; Hvojnik, M.; Mikula, M. The effect of the ink composition on the performance of carbon-based conductive screen printing inks. *J. Mater. Sci. Mater. Electron.* **2019**, *30*, 1034–1044. https://doi.org/10.1007/s10854-018-0372-7.
43. Ahmed, S.F.; Hasan, A.R. Rheology of low-rank coal-water slurries at both high and low shear rates. *Fuel* **1993**, *72*, 763–769. https://doi.org/10.1016/0016-2361(93)90077-F.